JOURNAL OF MATERIALS SCIENCE 25 (1990) 1751–1761

# Environmental shear deformation zones and crazes in crosslinked polystyrene and poly(*para*-methylstyrene)

PHILIP MILLER, EDWARD J. KRAMER
*Department of Materials Science and Engineering and the Materials Science Center, Cornell University, Ithaca, New York 14853, USA*

Thin films ($\sim 1\,\mu m$) of polystyrene and poly(*para*-methylstyrene) were bonded to annealed copper grids and crosslinked using electron radiation to increase $v$, the network strand density. At each $v$ separate films were strained in air and in Freon 113 until the critical strain, $\varepsilon_c$, for plastic deformation was reached. Transmission electron microscopy observations reveal that both sets of films undergo a transition from crazing to localized shear deformation zones (DZs) as $v$ is increased. The critical strains for both crazing and DZ formation are markedly decreased in Freon 113. The DZs formed in Freon 113 show abrupt changes in extension ratio, $\lambda$, at their interfaces while those formed in air show more diffuse changes in $\lambda$. A mechanism for environmental DZ formation is proposed in which the diffusion rate of Freon 113 into the DZ is strongly enhanced by the ongoing plastic deformation. This mechanism is suggested by Rutherford backscattering measurements of Freon 113 diffusion into PS which show that such diffusion in the absence of plastic deformation is much too slow to allow the observed rate of growth of the environmental DZs.

## 1. Introduction

### 1.1. Background

Polymeric materials are being used in greater amounts in a variety of applications. The weight savings and increased strength that polymers can offer make them extremely attractive to the transportation industry. The computer industry is demanding greater amounts of high performance polymers for the processing and packaging of semiconductor devices. The low cost, ease of processing and low diffusivity of polymers make them ideal for food containers, too.

As a result of the widespread use of polymers, they are being exposed to an increasing variety of harsh and exotic environments. An automobile part may come in contact with any number of organic fuels, hydraulic fluids and lubricants. Structural polymers in aircraft must withstand temperature changes of several hundred degrees. The failure of polymeric materials due to their environment must be foreseen and prevented. A common problem of thermoplastic polymers is the growth of cracks at very low stresses in the presence of an organic environment [1–4].

It is widely accepted that environmental stress cracking in thermoplastics involves the nucleation, growth and catastrophic breakdown of crazes to form cracks. In order to guard against environmentally induced failure, a better understanding of plastic deformation of polymers within an environment is needed.

This paper examines the plastic deformation of thin crosslinked films of polystyrene (PS) and poly(*para*-methylstyrene) (PPMS) in air and in Freon 113* (1,1,2-trichloro-1,2,2-trifluoroethane), a common industrial fluid. The mode and character of plastic deformation is related to the environment and strand density of the sample. The well-defined shoulders of environmental deformation zones are explained in the light of enhanced diffusion of Freon 113 into the plastically deformed material of the deformation zone. The critical strain for plastic deformation and the extension ratio of the plastically deformed regions strained in air and Freon 113 are reported and correlated with the strand density of the sample.

### 1.2. Competition between crazing and the formation of shear deformation zones

Thin polymer films strained in tension exhibit two modes of plastic deformation: crazing and the formation of shear deformation zones [5, 6]. Crazes are localized regions of plastic deformation that look like cracks optically, but unlike true cracks, crazes can support a load due to fibrils of highly drawn polymer which span the two craze/bulk interfaces. The typical fibril diameter in a craze is from 5 to 30 nm and the average fibril spacing is approximately from 15 to 60 nm depending on growth conditions [1–3, 6].

Crazes typically nucleate from defects which act as stress concentrators. Craze tip advance has been modelled by the Taylor meniscus instability mechanism [6, 7]. In this model, the strain softened material

*Freon is a registered trademark of E. I. du Pont de Nemours & Co.

0022–2461/90 $03.00 + .12 

just ahead of the craze tip is described as a non-Newtonian fluid. Fibrils formed as instabilities within the fluid meniscus leave behind finger-like voids as the meniscus advances. Air-grown crazes widen by drawing new materal into the fibrils from the active zone, a region of strain-softened material at the craze/bulk interface of $\sim 25$ nm wide [8]. Using a phantom fibril model, one can show that approximately one half of the polymer strands in the craze must break or disentangle during fibrillation [9].

The second type of plastic deformation that occurs in thin films strained in tension is the formation of shear deformation zones (DZs). DZs, in contrast to crazes, are regions of uniformly drawn polymer that do not contain any voids. DZs form by the realignment of short chain segments smaller than the entanglement length.

DZs nucleate at local inhomogeneities which act as stress concentrators. Initially, the material inside the DZ strain softens. As the polymer strands in the DZ align due to the applied stress, the polymer strain hardens. When the flow stress of the material in the DZ is greater than the applied stress further plastic deformation can only be accommodated by drawing new material at the DZ shoulders. This process, which is similar to necking in fibres, leads to a structure of uniformly drawn material inside the DZ with shoulders of material drawn to decreasing stages of extension [10–12]. These structures appear diffuse by transmission electron microscopy (TEM) [13].

It has been found that the natural entanglement density, $\nu_e$, will determine which mode of deformation a polymer film will undergo when strained in tension [5, 6]. Polymers with low entanglement densities such as PS ($\nu_e = 3.3 \times 10^{25}$ strands m$^{-3}$) craze, whereas high entanglement density polymers such as polycarbonate ($\nu_e = 29.0 \times 10^{25}$ strands m$^{-3}$) typically form DZs. Polymers such as poly(styrene–acrylonitrile) with intermediate values of $\nu_e$ ($\nu_e = 10.1 \times 10^{25}$ strands m$^{-3}$) can exhibit both types of deformation [5, 6]. Adding chemical crosslinks increases the strand density of a polymer [14] and well below the glass transition temperature, $T_g$, entanglements act as permanent crosslinks. Thus, below $T_g$, the entanglement density and the crosslink density, $\nu_x$, are additive and the total strand density, $\nu$, can be written as

$$\nu = \nu_e + \nu_x \tag{1}$$

The work to create a new surface during fibrillation, $\Gamma$, can be written as [6]

$$\Gamma = \gamma + \tfrac{1}{4} U_b \nu d \tag{2}$$

where $\gamma$ is the van der Waals surface energy of intermolecular separation, $U_b$ is the energy required to break a main chain bond and $d$ is the mesh size or end-to-end vector distance between entanglements. For uncrosslinked PS strained in air the two terms are nearly equal in magnitude: $\gamma \approx 40$ mJ m$^{-2}$ and $\frac{1}{4} U_b \nu d \approx 47$ mJ m$^{-2}$. As the crosslink density is increased the second term in Equation 1 will dominate and $\Gamma$ will increase. At large enough strand densities, the energy to create new fibril surfaces will be prohibitive and the formation of shear formation zones will be favoured.

### 1.3. Extension ratio

Two other physical parameters which are related to the strand density are the strand contour length and the network mesh size. The contour length, $l_e$, is given by

$$l_e = \left(\frac{l_0}{M_0}\right)\left(\frac{\varrho N_A}{\nu}\right) \tag{3}$$

where $l_0$ is the length of the fully extended repeat unit, $M_0$ is the molecular weight of the repeat unit, $\varrho$ is the density of the polymer and $N_A$ is Avogadro's number. The mesh size or end-to-end vector distance, $d$, between entanglements is given by

$$d = k\left(\frac{\varrho N_A}{\nu}\right)^{1/2} \tag{4}$$

where $k$ is a constant of proportionality and may be determined from measurements of the molecular coil size.

If there is no chain scission or disentanglement, the maximum extension a polymer strand can undergo, $\lambda_{max}$, can be written as [6]

$$\lambda_{max} = \frac{l_e}{d} \tag{5}$$

Typically, the extension ratio measured experimentally, $\lambda$, never reaches the calculated value of $\lambda_{max}$. Strain hardening of plastically deformed material raises the flow stress above the applied stress and the polymer strands never become fully aligned. Empirically, it is found that $\lambda_{craze} = 0.9\lambda_{max}$ and $\lambda_{DZ} = 0.6\lambda_{max}$ [14–16]. The extension ratio of a craze is larger than the extension ratio of a DZ because chains broken during fibrillation allow the polymer strands in crazes to be drawn to higher extensions than the strands in DZs.

## 2. Experimental procedure

### 2.1. Mechanical properties

Nearly monodisperse PS of molecular weight, $M_w = 390\,000$ which had a polydispersity index $M_w/M_n < 1.2$ was purchased from the Pressure Chemical Company. Polydisperse PPMS of molecular weight $M_w = 418\,000$ was provided by the Mobil Chemical Company. The polydispersity was measured with a Waters gel permeation chromatograph and it was determined that $M_w/M_n = 2.9$ [17].

Thin films of the polymers were cast on glass slides by drawing them at a constant rate from a toluene solution. The films were determined to be approximately 0.9 $\mu$m thick as measured by a Zeiss interference microscope. After the toluene had evaporated, the films were cut into rectangular sections and floated off the slides onto the surface of a water bath. The sections were picked up on annealed copper grids, the grid bars of which had been previously coated with the appropriate polymer. A brief exposure to toluene vapour bonded the films to the copper grids.

The samples were examined with an optical microscope and a suitable film square was selected which

contained few dust particles and no large defects. This film square was crosslinked by rastering the electron beam of a JEOL 733 electron microprobe across the sample. The electrons were accelerated to 40 kV with a beam current of $1 \times 10^{-7}$ A. The beam was defocused to a diameter of 0.4 mm and the total area rastered across the sample was approximately 8 $mm^2$ (the equivalent of about four film squares). Samples that were used for the extension ratio measurements had starter cracks burnt into them with a focused electron beam prior to irradiation [13].

The gel dose was determined by irradiating selected film squares for various times. The samples were placed in a toluene bath to dissolve any uncrosslinked sol fraction and then placed successively in acetone and methanol baths to extract the trapped solvent in the fragile gel fraction. Once the samples were dry, they were examined with an optical microscope to determine whether or not any crosslinked film remained.

Statistically, there is one crosslink per molecule in the film at the gel point [18]. Although every molecule may not be crosslinked into the network, a film irradiated with the gel dose should not dissolve completely in the toluene bath. Samples of PS which were irradiated for times less than 43 sec invariably dissolved, whereas films which had been irradiated for more than 47 sec typically survived immersion in toluene. In this manner, it was determined that an irradiation time of 45 sec would crosslink the sample to its gel point. This gel time, $t_{gel}$, corresponds to an incident dose of $5 \times 10^{-7}$ C $mm^{-2}$. This result is in reasonable agreement with the gel dose found by Henkee and Kramer [14], who determined the gel dose of PS by measuring the thickness of the gel fraction and constructing a Charlesby–Pinner plot [19]. The gel time for PPMS was determined in the same fashion. The crosslinked strand density, $\nu_x$, of the sample was calculated from the expression

$$\nu_x = t_{irr} \frac{N_A \varrho}{M_w} \frac{1}{t_{gel}} \tag{6}$$

where $t_{irr}$ is the irradiation time, $N_A$ is Avogadro's number, $\varrho$ is the density of the polymer and $M_w$ is the molecular weight of the polymer.

The samples were allowed to stand for 24 h after they had been irradiated to the desired crosslink density. The grids were then clamped to a strain frame and mounted over an optical microscope. To measure the critical strain for deformation in air, $\varepsilon_c$(air), the samples were slowly strained by hand until plastic deformation was first observed. The Freon 113 environmental samples were strained incrementally in air and a drop of Freon 113 was gently deposited on the surface of the film after each strain step until plastic deformation was observed. In this manner, the critical strain for deformation in Freon 113, $\varepsilon_c$ (Freon 113), was determined.

Because of the low magnification of the optical microscope, crazes and DZs could not be distinguished from dust particles until they grew to a critical size (*ca.* 50 $\mu$m long). (The critical size for detecting DZs grown in high strand density samples was slightly larger due to their diffuse nature.) Thus, the values measured for $\varepsilon_c$ were indicative of craze or DZ growth and not craze or DZ nucleation.

The extension ratios of shear deformation zones and crazes were measured using the following procedure. The sample was strained an additional 1 or 2% beyond $\varepsilon_c$ to create a wide craze or DZ. The irradiated film square was carefully cut from the sample and observed in a JEOL 200CX transmission electron microscope at an accelerating voltage of 200 kV. Micrographs were taken of the craze or DZ and of the hole that had been burnt into the film. These micrographs were then examined with a Joyce–Loebl Microdensitometer 6 to measure the optical density, $\Phi$, of these regions.

The thickness fraction or volume fraction of polymer in the plastically deformed region, $\nu_f$, was determined from [20]

$$\nu_f = 1 - \frac{\ln (\Phi_{craze}/\Phi_{film})}{\ln (\Phi_{hole}/\Phi_{film})} \tag{7}$$

where $\Phi_{craze}$ is replaced with $\Phi_{DZ}$ for films that exhibited deformation zones. If the total mass of the polymer in the deformed region remains unchanged after straining, one can determine the extension ratio, $\lambda$, of the craze or DZ from

$$\lambda = \frac{1}{\nu_f} \tag{8}$$

## 2.2. Diffusion measurements

A concentrated solution of PS in toluene was used to create thick films ($> 3\,\mu$m) for the measurement of diffusion of Freon 113 into PS with Rutherford backscattering spectrometry (RBS). Aluminium substrates which had been previously etched with an NaOH solution to roughen them were dipped into the PS/toluene solution and pulled out at a constant rate and allowed to dry. These samples were then placed for various times, $t$, in liquid Freon 113 at room temperature. When exposure was complete, the samples were quickly removed from the Freon 113 and submerged directly in liquid nitrogen to halt any further diffusion. The samples were transferred in a glove bag filled with dry nitrogen to prevent water vapour from condensing on the surface of the samples, into an evacuated RBS analysis chamber (pressure $< 10^{-6}$ torr) via a load lock. Liquid nitrogen was pumped through a cold stage sample mount to prevent the films from warming while the RBS spectra were collected.

Computer algorithms [21, 22] developed by Doolittle were used to simulate concentration profiles and these were compared with the collected RBS spectra. It was found that Freon 113 diffusing into PS is characterized by Case II diffusion which can be divided into two steps: (a) a transient swelling regime at short diffusion times during which the Case II diffusion front becomes established, and (b) once the Case II diffusion front has formed, a steady state regime in which the front velocity is a constant. A standard complementary error function solution for the concentration of a penetrant diffusing into an infinite medium of the form [23]

$$c(x, t) = c_0 \operatorname{erfc}\left[\frac{x}{2(Dt)^{1/2}}\right] \tag{9}$$

can be used to approximate the diffusion profile in the transient step of Case II diffusion, where $c_0$ is the initial concentration of the diffusant, $x$ is the distance from the surface of the sample and $D$ is the diffusion coefficient. In the steady state step, the concentration profile is described by

$$c(x_f, t) = c_0 \exp\left(-\frac{x_f v}{D}\right) \quad (10)$$

where $x_f$ is the distance ahead of the Case II front and $v$ is the velocity of the front [24, 25]. The diffusion coefficient was determined by varying the values of $c_0$ and $D$ until the simulation best fit the experimental data.

## 3. Results and discussion

### 3.1. Solvent diffusion and plasticization

Fig. 1a shows a typical Rutherford backscattering spectrum for PS exposed to liquid Freon 113 at room temperature for 527 100 sec. For an incident energy of $E_0 = 2.4$ MeV, chlorine, fluorine and carbon at the surface of an RBS sample appear at channel numbers 309, 207 and 122, respectively. The fluorine profile is lost in the background noise due to the relatively small scattering cross-section of this element. The small peak at channel number 175 is due to atoms of oxygen from water vapour that condensed on the sample surface during the transfer into the load lock.

Fig. 1b is an enlarged view of the chlorine peak in Fig. 1a. This diffusion profile corresponds to the transient regime of Case II diffusion and the concentration profile can be approximated using Equation 9. The solid line in Fig. 1b is a simulation of the diffusion profile where $D = 5 \times 10^{-15}$ cm$^2$ sec$^{-1}$.

Fig. 1c is an RBS spectrum of PS exposed to liquid Freon 113 for $9 \times 10^6$ sec. This sample is well into the steady-state regime of Case II diffusion. The Case II front has penetrated the sample to a depth of 730 nm and the front velocity is estimated to be $v \approx 3 \times 10^{-13}$ m sec$^{-1}$. The concentration of Freon 113 in the Case II front for this sample is determined to be $c_0 = 0.21$ (which is equivalent to a volume fraction $\phi = 0.15$). Since an identical Case II front concentration is determined for a sample exposed to Freon 113 for $3.9 \times 10^6$ sec, this value is taken as the equilibrium value of the concentration of Freon 113 in PS.

In practice it is difficult to measure the glass transition temperature, $T_g$, of PS plasticized with Freon 113. The boiling point of Freon 113 is 48° C [26], which is below the $T_g$ of the plasticized polymer. The glass transition cannot be measured using differential scanning calorimetry because the signal from Freon 113 boiling out of the sample overwhelms any signal from the glass transition. Mechanical tests to determine the $T_g$ of PS plasticized with Freon 113 typically require samples of at least several microns thick. It takes a prohibitively long time to saturate a thick PS film with Freon 113 since Freon 113 is such a slow diffusant; it would be necessary to soak a sample 3 $\mu$m thick for more than 100 days in Freon 113 to saturate it. Thus it is necessary to estimate $T_g$ of the plasticized polymer by theoretical means.

It is possible to estimate a value for $T_g$ of a plasticized polymer from the Kelley–Bueche equation [27] if the volume fraction of plasticizer is known. $T_g$ may be determined by

$$T_g = \frac{\alpha_p (T_g)_p (1 - \phi_s) + \alpha_s (T_g)_s \phi_s}{\alpha_p (1 - \phi_s) + \alpha_s \phi_s} \quad (11)$$

where $\alpha$ is the thermal expansion coefficient, $\phi$ is the volume fraction and the subscripts p and s stand for polymer and solvent respectively. The Kelley–Bueche equation is derived from a free volume treatment of $T_g$ and is only accurate for $\phi_s < 0.2$. Substituting values of $\alpha_p = 5.5 \times 10^{-4}$ K$^{-1}$, $\alpha_s = 1.4 \times 10^{-3}$ K$^{-1}$, $(T_g)_p = 373$ K, $(T_g)_s = 238$ K and $\phi_s = 0.15$, determined from RBS spectroscopy, into Equation 11, gives a value for the glass transition temperature of PS plasticized by Freon 113 of $(T_g)_{\text{plasticized}} = 58°$ C [28, 29].

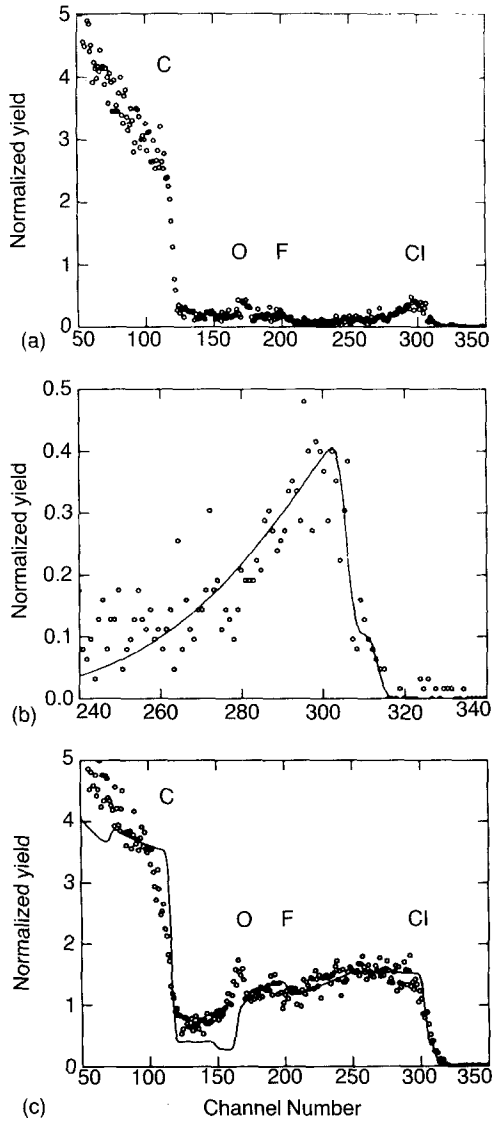


*Figure 1* Rutherford backscattering spectra of PS into which Freon 113 has been diffused at room temperature. (a) Diffused 527 100 sec. (b) An enlarged view of the chlorine peak in (a), the solid line corresponds to a concentration profile simulation using a diffusion coefficient $D = 5 \times 10^{-15}$ cm$^2$ sec$^{-1}$. (c) Diffused $1.9 \times 10^6$ sec, the solid line corresponds to a concentration profile simulation using a diffusion coefficient $D = 5 \times 10^{-15}$ cm$^2$ sec$^{-1}$ and a Case II front velocity $v = 3 \times 10^{-13}$ m sec$^{-1}$.

### 3.2. Craze and DZ microstructure

The plastic zones produced by tensile deformation of

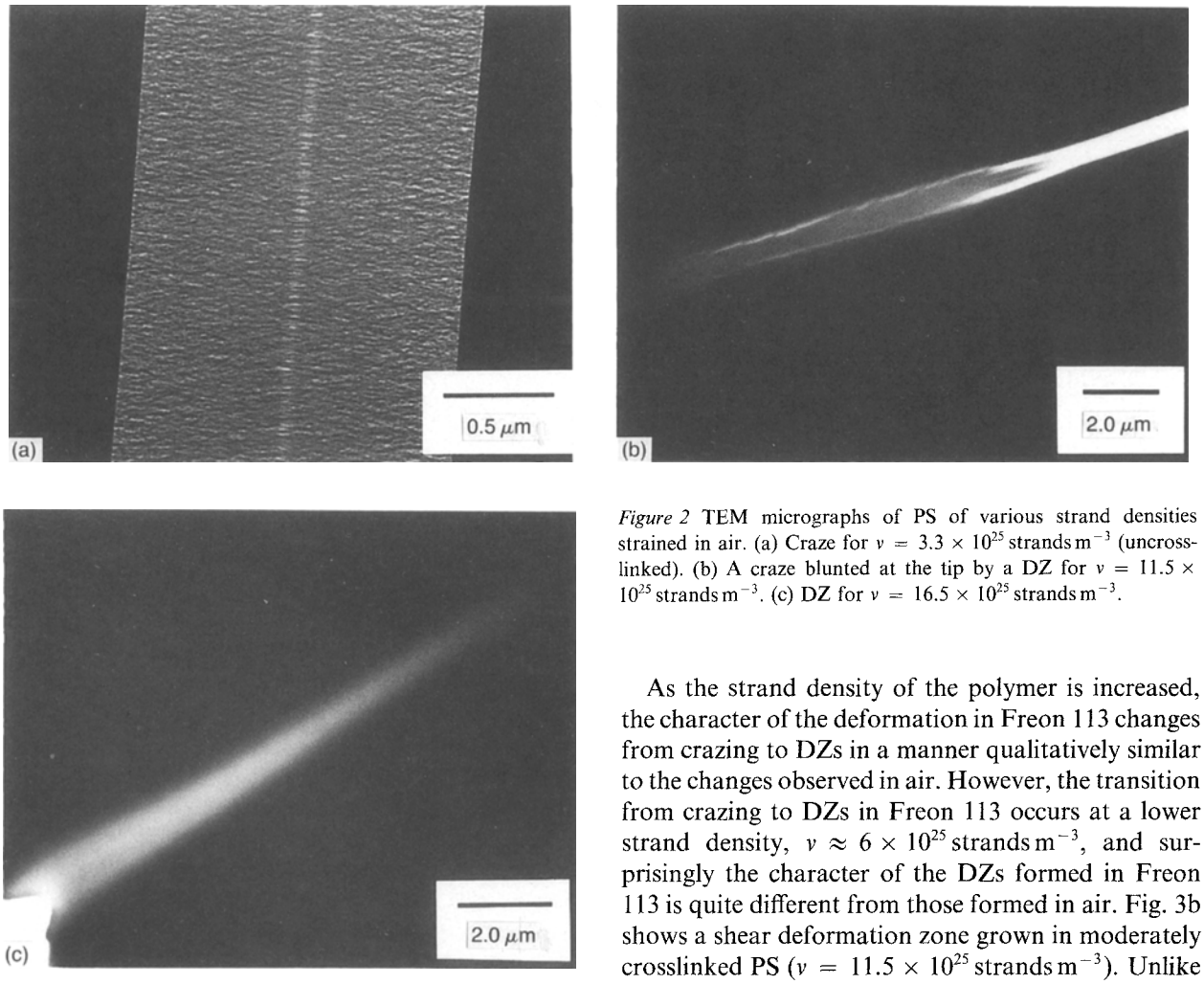


*Figure 2* TEM micrographs of PS of various strand densities strained in air. (a) Craze for $\nu = 3.3 \times 10^{25}$ strands $m^{-3}$ (uncrosslinked). (b) A craze blunted at the tip by a DZ for $\nu = 11.5 \times 10^{25}$ strands $m^{-3}$. (c) DZ for $\nu = 16.5 \times 10^{25}$ strands $m^{-3}$.

PS in air change character from crazes to shear deformation zones as the network strand density is increased [16]. These changes are illustrated in the micrographs in Figs 2a to c. Fig. 2a shows the typical microstructure of a craze grown in uncrosslinked PS ($\nu = 3.3 \times 10^{25}$ strands $m^{-3}$) strained in air. The fibrils that span the craze/bulk interface are easily distinguished. The craze midrib, a localized zone of high extension that forms in the region of high stress concentration just behind the craze tip, is evident at the centre of the craze.

The nature of the plastic deformation changes as the total strand density is increased. Initially, the craze tips are blunted by plane stress shear deformation zones (Fig. 2b, $\nu = 11.5 \times 10^{25}$ strands $m^{-3}$). At higher values of $\nu$, all crazing is suppressed and plastic deformation occurs by shear deformation zones (Fig. 2c, $\nu = 16.5 \times 10^{25}$ strands $m^{-3}$). These shear deformation zones become increasingly more diffuse as the strand density increases. Similar features are observed for the PPMS films.

Straining the PS and PPMS samples in Freon 113 significantly alters the nature of the plastic zones. Fig. 3a is a micrograph of a craze grown in Freon 113 in uncrosslinked PS ($\nu = 3.3 \times 10^{25}$ strands $m^{-3}$). The fibrils in this craze have collapsed together and appear coarser than those of crazes grown in air. The fibril structure collapse and coarsening is due to forces exerted on the fibrils by the air–Freon 113 meniscus during drying of the craze [30].

As the strand density of the polymer is increased, the character of the deformation in Freon 113 changes from crazing to DZs in a manner qualitatively similar to the changes observed in air. However, the transition from crazing to DZs in Freon 113 occurs at a lower strand density, $\nu \approx 6 \times 10^{25}$ strands $m^{-3}$, and surprisingly the character of the DZs formed in Freon 113 is quite different from those formed in air. Fig. 3b shows a shear deformation zone grown in moderately crosslinked PS ($\nu = 11.5 \times 10^{25}$ strands $m^{-3}$). Unlike DZs grown in air, these environmental DZs have well-defined shoulders. Fig. 3c reveals the sharp tip typical of a DZ grown in Freon 113. Deformation zones with these features are *never* seen in samples strained in air.

Because of these sharp edges, environmental DZs look exactly like crazes under the optical microscope. Fig. 4a is an optical micrograph of a single film square of a PS sample. The region designated by the arrows is a strip of crosslinked material with strand density of $\nu = 16.5 \times 10^{25}$ strands $m^{-3}$. This sample was strained in Freon 113 and several regions of plastic deformation have grown from the uncrosslinked region into the crosslinked strip. As illustrated in Fig. 4a, the crazes in the uncrosslinked region of the film appear identical to the environmental DZs in the crosslinked strip. In order to prove that the environmental DZs grown in Freon 113 are actually regions of unfibrillated shear deformation and not crazes whose fibrils have completely coalesced in the Freon 113, it is necessary to examine the plastic zones by TEM.

Figs 4b to d are transmission electron micrographs which correspond to the points A, B, and C of Fig. 4a, respectively. Fig. 4b clearly shows the fibrillar structure of an environmental craze of the type seen in Fig. 3a. This micrograph is from a region well outside the crosslinked strip. Fig. 4c shows the typical microstructure observed as one follows the craze into the crosslinked strip. The voids are isolated and begin to disappear entirely as the plastically deformed region enters the crosslinked strip. Only an unfibrillated zone

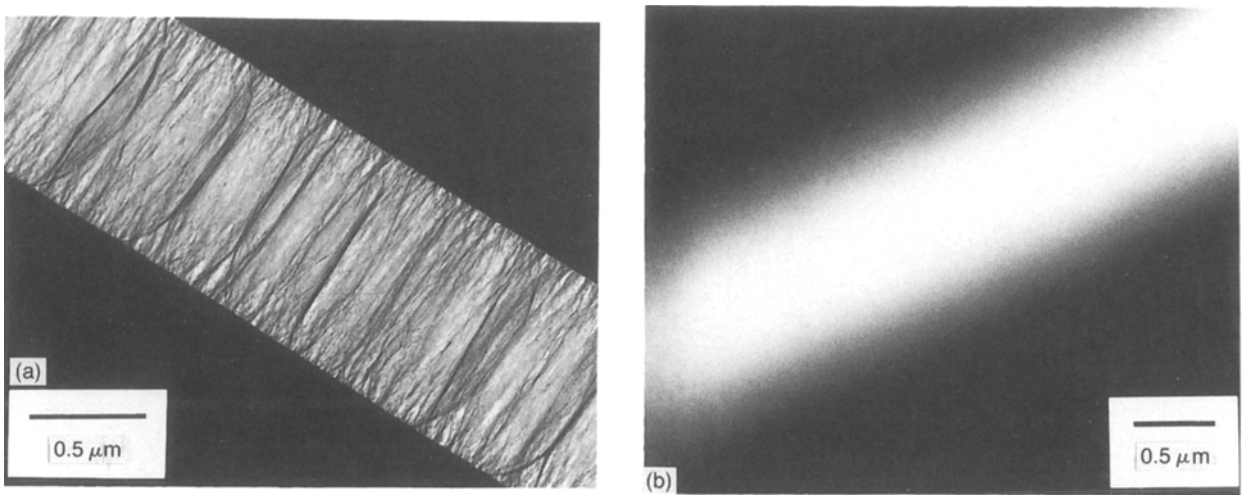


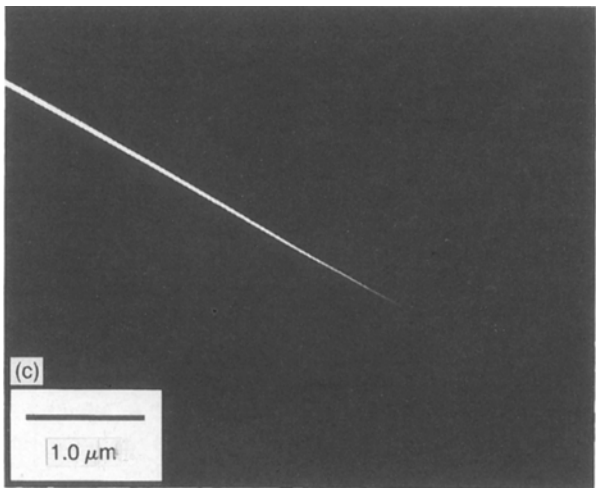


*Figure 3* TEM micrographs of PS strained in Freon 113. (a) Craze, $v = 3.3 \times 10^{25}$ strands $m^{-3}$. (b) DZ (body) for $v = 11.5 \times 10^{25}$ strands $m^{-3}$. (c) DZ (tip) for $v = 11.5 \times 10^{25}$ strands $m^{-3}$.

of plastic deformation is observed inside the crosslinked strip (Fig. 4d). Since craze fibrils are evident in Fig. 4b and only disappear within the crosslinked strip, it is clear that fibril coalescence cannot account for the unfibrillated structure in Fig. 4d. The structures in Figs 3b and 4d are true environmental shear deformation zones.

### 3.3. The transition from crazes to DZs

The transition from the formation of crazes to the formation of shear deformation zones shifts to lower values of $v$ in the Freon 113 environment. Only crazing is evident for PS strained in air at strand densities less than $7 \times 10^{25}$ strands $m^{-3}$. The transition region, where both crazes and shear deformation zones are present, occurs between $7 \times 10^{25}$ and $12 \times 10^{25}$ strands $m^{-3}$. For strand densities greater than $12 \times 10^{25}$ strands $m^{-3}$ only shear deformation zones are evident. (Henkee and Kramer [14] found the transition region for PS strained in air was between $4 \times 10^{25}$ and $8 \times 10^{25}$ strands $m^{-3}$. Slight differences in the measured value of $t_{gel}$ can account for the discrepancy in the transition region as determined in this paper.) Straining PS samples in Freon 113 shifts the transition region to between $6 \times 10^{25}$ and $8 \times 10^{25}$ strands $m^{-3}$. Likewise, the transition region is shifted in PPMS to lie from $6 \times 10^{25}$ to $14 \times 10^{25}$ strands $m^{-3}$ for samples strained in air to $4 \times 10^{25}$ to $5 \times 10^{25}$ strands $m^{-3}$ for samples strained in Freon 113.

From Equation 2 it is clear that the energy to create new fibril surfaces, $\Gamma$, will increase as the strand density increases. If $\Gamma$ becomes too large, crazing will not be favoured energetically. More exactly, one can show that the stress required to widen a single isolated craze, $S_C$, is given by [6]

$$S_c \propto [(\sigma_y)^* \Gamma]^{1/2} \tag{12}$$

where $(\sigma_y)^*$ is the yield stress of the strain-softened material in the active zone and $\Gamma$ is the energy required to create a new fibril surface as described by Equation 2. Substituting the expression for $d$ from Equation 4 into Equation 2 yields

$$\Gamma = \gamma + cv^{1/2} \tag{13}$$

where $c$ is a constant. From Equations 12 and 13 one can write

$$S_c \propto [(\sigma_y)^*]^{1/2} [\gamma + cv^{1/2}]^{1/2} \tag{14}$$

The stress to propagate a DZ, $S_{DZ}$, is proportional to the yield stress, $\sigma_y$, and should not depend upon the strand density of the polymer since DZs widen by the realignment of polymer segments smaller than the strand length. Thus,

$$S_{DZ} \propto \sigma_y \tag{15}$$

Fig. 5 is a plot of log $S_c$ and log $S_{DZ}$ as a function of log $v$. At low values of $v$, $S_c < S_{DZ}$ and crazing is the dominant mode of plastic deformation; at large values of $v$, $S_c > S_{DZ}$ and DZs are favoured. The transition from crazing to the formation of DZs occurs at a value of $v$ where the two curves cross, $v_t$.

If the sample is crosslinked to a value slightly less than $v_t$ crazing will be the dominant mode of deformation. However, the higher stresses at the craze tip may be enough to cause shear deformation zones to grow in place of a normal craze midrib [31]. Samples that are crosslinked to values slightly greater than $v_t$ may initially form crazes. As the craze grows, the stress on the sample is relaxed due to the plastic yielding and DZs will become the dominant mode of plastic deformation. Thus samples with $v$ slightly greater than $v_t$

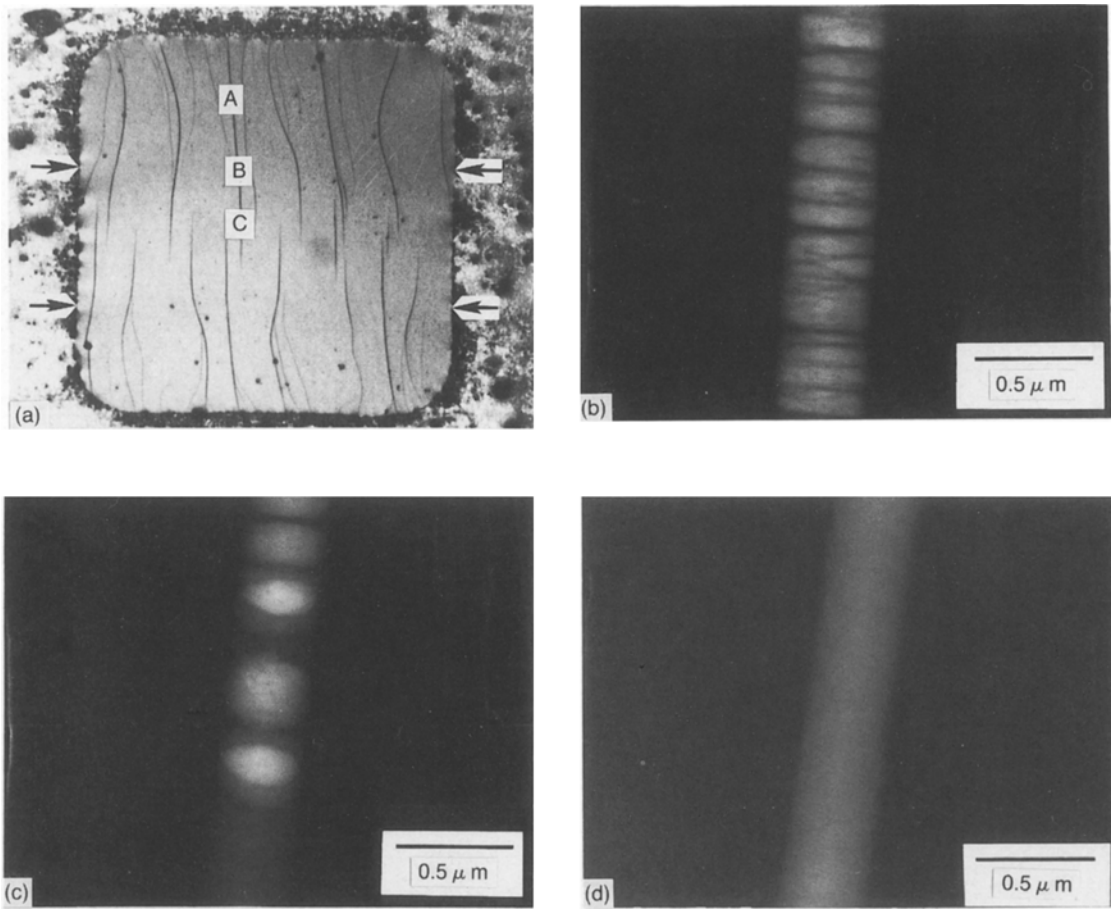


*Figure 4* (a) An optical micrograph of sample strained in Freon 113 containing a strip of crosslinked material (arrows) with $\nu = 16.5 \times 10^{25}$ strands $m^{-3}$. (b) TEM micrograph of a craze from region A. (c) TEM micrograph of a craze/DZ region from the edge of the crosslinked strip, region B. (d) TEM micrograph of a DZ from region C.

will produce a craze ending in a blunt DZ tip like that of Fig. 2b.

The dashed lines in Fig. 5 represent the stress required for the plastic deformation of samples strained in Freon 113. As can be seen in Equation 12, there are two contributions to $S_c$: a yield stress term and a surface energy term. The effects of the Freon 113 environment on the surface energy term are only significant at low strand densities. Although a Freon 113 environment will reduce $\gamma$ (Freon 113 wets the surface of PS), this contribution becomes less important at larger strand densities where the second term in Equation 2 dominates the behaviour of $\Gamma$. Since even a moderate amount of crosslinking will trap entanglements, it is unlikely that disentanglement will reduce $\nu$ and decrease $S_c$ in all but lightly crosslinked samples.

The plasticization effect of Freon 113 will decrease the yield stress term in Equation 12 regardless of the sample strand density. Thus, at low strand densities the reduction in $\Gamma$ and $(\sigma_y)^*$ will both contribute to the decrease in $S_c$, while at moderate and high strand densities, only the reduction in $(\sigma_y)^*$ will decrease $S_c$. Since the stress to propagate a DZ is directly proportional to $\sigma_y$. $S_{DZ}$ is reduced in the Freon 113 environment by an amount $[(\sigma_y)\text{air} - (\sigma_y)\text{Freon}]$ which is independent of the strand density. As seen in Fig. 5, since the decrease of $S_{DZ}$ is greater than the decrease of $S_c$ in the environment, the transition region is shifted to lower values of $\nu$.

## 3.4. Critical strain for deformation

Increasing the total strand density of the polymer also increases the total strain necessary to cause plastic deformation. Fig. 6a shows the critical strain, $\varepsilon_c$, necessary to plastically deform PS in air, as a function of the total strand density. The open circles are data from samples that plastically deformed only by crazing, the solid circles are data from samples that only formed shear deformation zones, and the half-filled circles are data from samples that exhibited both types of plastic deformation. Fig. 6b is a similar plot for PPMS samples.

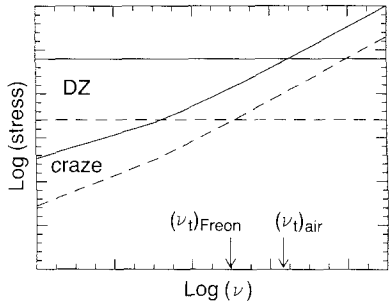


*Figure 5* Plot of the logarithm of stresses for crazing $S_C$ and for DZ formation as a function of the logarithm of strand density (in arbitrary units) in air (solid lines) and Freon 113 (dashed lines). It was assumed that $(\sigma_y)^* = \sigma_y = 600$ in air and $(\sigma_y)^* = \sigma_y = 300$ in Freon 113. The constant $c$ in Equation 14 was set to 22, and it was assumed that $\gamma = 40$ in air and 20 in Freon 113.

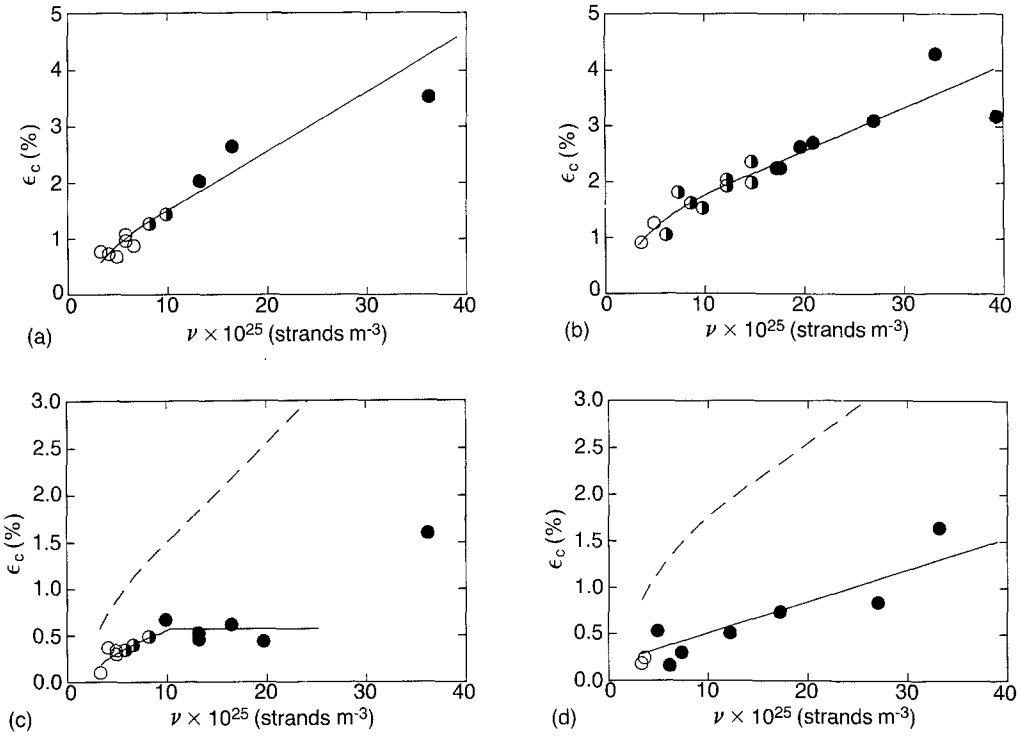


*Figure 6* The critical strain for plastic deformation as a function of strand density for (a) PS strained in air, (b) PPMS strained in air, (c) PS strained in Freon 113 and (d) PPMS strained in Freon 113. The dashed lines in (c) and (d) represent the values of $\varepsilon_c$ for PS and PPMS, respectively, strained in air.

In air, the two polymers behave in a qualitatively similar manner over the entire range examined. The $\varepsilon_c$ is approximately 0.007 for both uncrosslinked polymers which is consistent with previous results [32]. The critical strain for crazing and the critical strain for the formation of DZs both increase with $\nu$ over the entire range examined. At the highest values of $\nu$, neither PS nor PPMS show any plastic deformation until strains greater than 0.03 are reached. Since air-grown DZs become more diffuse as the strand density of the sample is increased, they are more difficult to detect optically. These samples must be strained to greater values in order for the DZs to be detectable, and therefore the values of $\varepsilon_c$ for highly crosslinked samples are likely to be larger than the true values for DZ initiation. This systematic error should increase with increasing $\nu$.

As expected, the presence of the Freon 113 environment greatly reduces the strain necessary for the formation of crazes in these polymers. Fig. 6c and d are the plots for PS and PPMS strained in Freon 113, respectively. Again, the open circles are data from samples that only formed crazes, the solid circles are data from samples that only formed shear deformation zones, and the half-filled circles are data from samples that exhibited both types of plastic deformation. For comparison, the curves from PS and PPMS strained in air are represented by the dashed lines. Since environmental DZs are easy to observe by optical microscopy (except for samples with extremely high crosslink densities), the values for $\varepsilon_c$ for samples strained in Freon 113 do not contain the systematic error associated with the samples strained in air.

The linear relationship between stress and strain strictly holds only in the elastic region of a stress–strain curve. If the total amount of plastic deformation is small, one may approximate the relationship between stress and strain as linear. This is a reasonable approximation for crazes and DZs, and thus $\varepsilon_c$(craze) and $\varepsilon_c$(DZ) should be proportional to $S_c$ and $S_{DZ}$, respectively, and the trends displayed in Fig. 5 should be reflected in the strain against strand density curves.

Uncrosslinked films of PS and PPMS strained in Freon 113 craze at very small strains ($< 0.001$), critical strains that are approximately a factor of $\sim 7$ smaller than the critical strain in air. (The uncrosslinked samples crazed immediately upon adding the Freon 113 during some of the tests. It is thought in these cases that the small stresses created from clamping the sample to the strain frame or from the weight of the Freon 113 droplet on the film were enough to craze the film without any additional strain being applied.) As the strand density is increased this factor decreases to $\sim 3$ at the value of $\nu$ where the transition from crazing to the formation of shear deformation zones occurs. As shown in Fig. 5, the additional decrease in $S_c$ due to the reduction of $\Gamma$ at low crosslink densities accounts for the qualitatively large differences in $\varepsilon_c$(air) and $\varepsilon_c$(Freon 113) at small values of $\nu$.

Although the RBS experiments indicate that Freon 113 is a slow diffuser, remarkably the critical strain necessary to form a DZ is substantially decreased in Freon 113 from its value in air as shown in Figs 6c and d. From Fig. 5 it is apparent that if $S_{DZ}$ were not reduced in the Freon 113 environment, then the transition from crazes to DZs would occur at larger values of $\nu$ than samples strained in air. Clearly, this is not the case. These data show convincingly that the Freon 113 environment must penetrate and plasticize the actively deforming polymer in the environmental DZs.

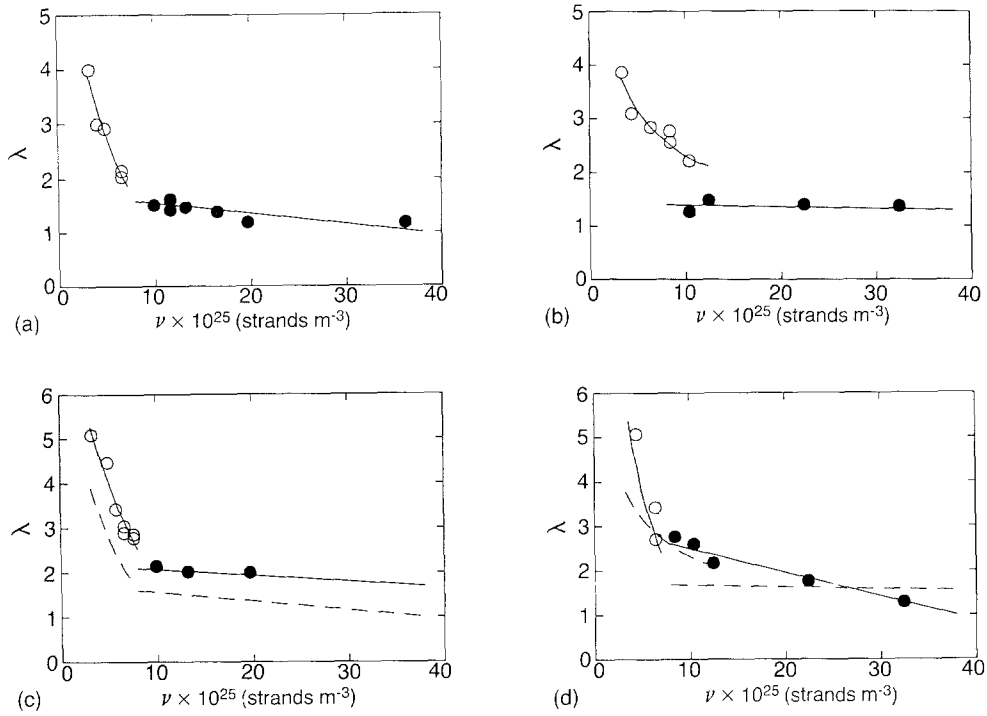


*Figure 7* The extension ratio of crazes (open circles) and DZs (filled circles) against the strand density for (a) PS strained in air, (b) PPMS strained in air, (c) PS strained in Freon 113 and (d) PPMS strained in Freon 113. The dashed lines in (c) and (d) represent the values of $\lambda$ for PS and PPMS, respectively, strained in air.

## 3.5. Extension ratios

The extension ratio, $\lambda$, is a measure of the natural elongation of the molecular chains in the plastic zone. Fig. 7a is a plot of the extension ratio against strand density for PS strained in air. The open circles represent the extension ratios of the PS crazes; the solid circles represent the data from the shear deformation zones. The value for extension ratios measured in crazed regions of PS drops sharply as a function of the strand density. There is a discontinuity between the crazing curve and the curve describing the extension ratios of the shear deformation zones. The extension ratios measured in regions of shear deformation only decrease slightly with increasing strand density. Qualitatively, similar results are found for PPMS (Fig. 7b).

When the samples were strained in a Freon 113 environment it is found that the extension ratios are consistently larger for both PS (Fig. 7c) and PPMS (Fig. 7d) over the entire range of $\nu$. As in the previous two plots, the open circles correspond to data from crazed regions while the solid circles represent data from shear deformation zones. For comparison the dashed line in these figures represents the data from samples strained in air.

The process of crazing invariably breaks main chain bonds as the polymer strands are drawn into the fibrils in PS and PPMS. Only about half of the polymer strands in a craze survive the fibrillation process in PS [9]. No strands are broken during the formation of a shear deformation zone which only involves the alignment of polymer segments shorter than the strand contour length. Because the effective strand density in the craze fibrils is reduced due to chain scission, the extension ratio of a craze is greater than the extension ratio of a DZ. Therefore, the discontinuity of $\lambda$ from crazes to DZs is due to the modification of the polymer network by the strand loss associated with craze fibril surface formation.

Although Freon 113 may enhance the disentanglement of strands during crazing [33] of the uncrosslinked samples, this mechanism cannot explain the uniform increase in $\lambda$ for entire range of $\nu$ examined since even a few crosslinks will inhibit disentanglement. Freon 113 reduces the yield stress of the polymer by plasticizing it and thus the material in the plastic zone will start deforming at smaller stresses. In addition, it is likely that the presence of a plasticizer reduces the required stress for the reorientation of polymer strands thus decreasing the strain hardening rate. Hence the polymer in an environmental craze or DZ will be drawn to larger extensions than in samples strained in air.

## 3.6. Evidence for enhanced diffusion in shear deformation zones

The results from the critical strain and extension ratio measurements clearly indicate that polymer films strained in Freon 113 are plasticized. In addition, the change in DZ microstructure from those grown in air to those grown in Freon 113 strongly indicates that only the material inside the DZ is plasticized by the Freon 113. If the entire film were plasticized then one would expect to see diffuse DZs like those observed in samples strained in air. The well-defined shoulders of the environmental DZs imply that the bulk film is not plasticized.

The microstructures evident in Figs 3b, 3c and 4d can only be explained if Freon 113 is able to preferentially penetrate into the DZ and plasticize it. The environment would then only reduce the flow stress of the polymer inside the DZ; the bulk material would be unaffected and retain the high flow stress of the

unplasticized polymer. A deformation zone growing under such conditions would widen by the drawing of the plasticized polymer at the shoulder of the DZ. This mechanism would produce well-defined DZ shoulders and sharp tips.

The hypothesis that Freon 113 is only able to plasticize the material inside a DZ is consistent with the previously determined value for the diffusion coefficient of Freon 113 into undeformed PS. RBS experiments reveal that the diffusion of Freon 113 into bulk PS is very slow. At room temperature it would take nearly 12 days for Freon 113 to fully penetrate a film of PS 1 $\mu$m thick; the growth of DZs in Freon 113 occurs on a time scale of several seconds. It is possible to estimate a lower bound for the diffusion coefficient of Freon 113 into actively deforming polymer at the DZ shoulder from estimates of the diffusion time (the exposure time of the films to Freon 113, $\sim 1$ sec) and the diffusion length (the thickness of the DZ, $\sim 0.5\,\mu$m). This lower bound, $D$, is of the order of $10^{-8}$ to $10^{-9}$ cm$^2$ sec$^{-1}$ which is six to seven orders of magnitude larger than the diffusion coefficient found for Freon 113 penetrating into undeformed PS. The magnitude of this estimated diffusion coefficient is consistent with estimates of typical diffusion coefficients of organic solvents into oriented PS behind a Case II front [24, 25].

It is unlikely that a stress-enhanced diffusion mechanism could account for the extremely rapid diffusion into the plastic zone. It is known that the stresses at the plastic zone are slightly higher than the applied stress. The magnitude of the largest local stress, however, is less than a factor of two greater than the applied stress [6]. A stress-enhanced diffusion mechanism would have to contain a very strong dependence on stress in order to increase the diffusion rate by the six or seven orders of magnitude necessary to produce the type of environmental DZ observed. It is more likely that the environmental DZs are produced by a deformation-enhanced diffusion mechanism.

It is known that physically ageing a polymer will dramatically reduce the diffusion rate of organic solvents into the aged material, presumably due to the reduction of the polymer configurational entropy [24, 25]. Strain softening has the opposite effect on the polymer glass structure to physical ageing; strain softening rejuvenates the material and increases the polymer configurational entropy. Thus, it is reasonable that the diffusion of solvents into actively deforming polymer will be enhanced due to the strain softening that follows yield.

There is other evidence in literature that deformation-enhanced diffusion does occur. Kramer and Bubeck [34] inferred the enhanced diffusion of methanol into plastically deforming poly(methyl methacrylate) (PMMA). Harmon *et al.* [35] have also observed enhanced diffusion of methanol in plastically deformed PMMA.

Deformation-enhanced diffusion in crosslinked PS films would explain the microstructure of the environmental DZs observed in Figs 3b, 3c and 4d. The deformation-enhanced diffusion mechanism predicts that Freon 113 would preferentially diffuse into the actively deforming material in the DZ shoulder and lower its yield stress. Since it is known from the RBS data that Freon 113 will not substantially penetrate into undeformed PS, the material outside the DZ would retain the yield stress of the bulk PS film. This situation of having highly plasticized polymer surrounded by material with a greater yield stress, is necessary to produce the observed environmental DZ microstructures.

In summary, the evidence from critical strain and extension ratio measurements indicates that Freon 113 is able to readily plasticize PS and PPMS. RBS diffusion measurements of Freon 113 into undeformed PS reveal that Freon 113 diffuses six to seven orders of magnitude slower than is necessary to plasticize the PS films to produce the critical strain and extension ratio results that are observed. In addition, examination by TEM reveals that the environmental DZ microstructure is unlike that of air-grown DZs. This result indicates that the entire film is not plasticized by Freon 113; only the actively deforming polymer in the DZ is plasticized. Therefore, it is concluded that Freon 113 is preferentially able to penetrate into the DZ shoulder by a deformation-enhanced diffusion mechanism.

## 4. Conclusions

(1) Freon 113 diffuses slowly into bulk PS. The unusual nature of environmental DZs can be explained by the preferential diffusion of Freon 113 into the plastically deformed material at the DZ shoulders.

(2) Crazing is favoured energetically at low strand densities in thin films strained in tension; at high strand densities, the formation of shear deformation zones is the dominant mode of plastic deformation. The transition from crazes to DZs is shifted to lower values of $v$ for samples strained in Freon 113.

(3) The critical strain for plastic deformation increases as the total strand density of the polymer is increased. Freon 113 lowers $\varepsilon_c$ due to decreases in both $\Gamma$ and $\sigma_y$ in lightly crosslinked samples whereas only $\sigma_y$ is lowered significantly in moderately and highly crosslinked samples.

(4) The extension ratios of crazes are larger than those of DZs due the large amount of chain scission of the fibrillation process. Freon 113 uniformly increases the value of $\lambda$ over the entire range of $v$ examined, by reducing the yield stress of the polymer in the plastically deformed regions.

## Acknowledgements

The support of this work by the Cornell Materials Science Center which is funded by the National Science Foundation, DMR-MRL is gratefully acknowledged. Philip Miller was supported by a fellowship granted by the Mobil Chemical Company. The authors also wish to thank Dr Binnur Gunesin of the Mobil Chemical Company for providing the PPMS used in this work and W. Steinacker of du Pont for providing reference [29].

## References

1. A.N.GENT, in "The Mechanics of Fracture", AMD, Vol. 19, edited by F. Erdogon (ASME, New York, 1976) p. 55.

2. S. RABINOWITZ and P. BEARDMORE, *CRC Reviews* in *Macromol. Sci.* **1** (1972) 1.
3. R. P. KAMBOUR, *J. Polym. Sci. Macromol. Rev.* **7** (1973) 1.
4. E. J. KRAMER, in "Developments in Polymer Fracture", edited by E. H. Andrews (Applied Science Publishers, Barking, UK, 1979) p. 55.
5. A. M. DONALD and E. J. KRAMER, *Polymer* **23** (1982) 461.
6. E. J. KRAMER, in "Advances in Polymer Science 52/53" (Springer Verlag, Berlin, 1983) p. 7.
7. A. M. DONALD and E. J. KRAMER, *Phil. Mag.* **A43** (1981) 857.
8. P. MILLER, PhD thesis, Cornell University, New York (1987) Ch. 2.
9. C. C. KUO, S. L. PHOENIX and E. J. KRAMER, *J. Matr. Sci. Lett.* **4** (1985) 459.
10. A. S. ARGON, R. D. ANDREWS, J. A. GODRICK and W. WHITNEY, *J. Appl. Phys.* **39** (1968) 1899.
11. P. B. BOWDEN and S. RAHA, *Phil. Mag.* **22** (1970) 463.
12. E. J. KRAMER, *J. Polym. Sci., Polym. Phys. Ed.* **13** (1975) 509.
13. A. M. DONALD and E. J. KRAMER, *J. Mater. Sci.* **16** (1981) 2967.
14. C. S. HENKEE and E. J. KRAMER, *J. Polym. Sci., Polym. Phys.* **22** (1984) 721.
15. A. M. DONALD and E. J. KRAMER, *Polymer* **23** (1982) 1183.
16. *Idem, J. Polym. Sci.* **20** (1982) 899.
17. K. SHULL, private communication.
18. O. SAITO, in "The Radiation Chemistry of Macromolecules", edited by M. Dole (Academic Press, New York & London, 1972) p. 224.
19. A. CHARLESBY and S. H. PINNER, *Proc. R. Soc.* **A249** (1959) 367.
20. B. D. LAUTERWASSER and E. J. KRAMER, *Phil. Mag.* **39** (1979) 469.
21. L. R. DOOLITTLE, *Nucl. Inst. Meth.* **B9** (1985) 344.
22. *Idem, ibid.* **B15** (1986) 227.
23. J. CRANK, "The Mathematics of Diffusion", 2nd Edn (Clarendon Press, Oxford, 1983) p. 21.
24. H. COLL and C. G. SEARLES, *Polymer* **29** (1988) 1266.
25. R. C. LASKY, PhD thesis, Cornell University, New York (1986).
26. R. C. WEAST (ed.), "CRC Handbook of Chemistry and Physics", 63rd Edn (CRC Press, Boca Raton, FL, 1982) p. E-33.
27. F. N. KELLEY and F. BUECHE, *J. Polym. Sci.* **50** (1961) 549.
28. J. BRANDRUP and E. H. IMMERGUT (eds), "Polymer Handbook", 2nd Edn (John Wiley & Sons, New York, 1974) p. V-59.
29. "Thermodynamic Properties of 'Freon' 113 Trichlorotrifluoroethane $CCl_2F$–$CClF_2$ With Addition of Other Physical Properties" (du Pont de Nemours and Co, Wilmington, DE, 1985).
30. H. G. KRENZ, E. J. KRAMER and D. G. AST, *J. Mater. Sci.* **11** (1976) 2211.
31. L. L. BERGER, PhD thesis, Cornell University, New York (1986).
32. R. P. KAMBOUR, in "Mechanisms of Environment-Sensitive Cracking of Materials", edited by P. R. Swann, F. P. Ford and A. R. C. Westwood (Materials Society, London, 1977) p. 213.
33. L. L. BERGER and E. J. KRAMER, *Macromolecules* **20** (1988) 1980.
34. E. J. KRAMER and R. A. BUBECK, *J. Polym. Sci., Polym. Phys. Ed.* **16** (1978) 1195.
35. J. P. HARMON, S. LEE and J. C. M. LI, *J. Polym. Sci., Polym. Chem. Ed.* **25** (1987) 3215.

*Received 27 September 1988*
*and accepted 27 February 1989*